Case report

Chordoma with lung metastases at initial presentation of a pediatric patient

Samiat Agunbiade, MD[a], Ayman Nada, MD, Phd[a], Sudhir Bhimaniya, MD[b], Matthew T. Whitehead, MD[c,d], Eman S. Mahdi, MD[a,*]

[a] Department of Diagnostic Imaging and Radiology, University of Missouri Hospital/ Women's and Children's Hospital, Columbia, MO, USA
[b] Mallinckrodt Institute of Radiology, Washington University School of Medicine, St. Louis, MO, USA
[c] Department of Diagnostic Imaging and Radiology, Children's National Medical Center, Washington, DC, USA
[d] George Washington University Hospital, Washington, DC, USA

ARTICLE INFO

ABSTRACT

Chordomas are rare, slow growing malignant tumors derived from notochord remnants that can arise anywhere along the neuronal axis. Chordomas are particularly rare in patients under 20 years of age and tend to be intracranial in location, as opposed to sacrococcygeal in adults. Metastasis at initial presentation is uncommon in all age groups and is exceedingly rare in the absence of local recurrence of the primary tumor. We report a case of advanced clival chordoma with marked nasopharyngeal disease extension and lung metastases at the time of presentation in a pediatric patient.

© 2020 The Authors. Published by Elsevier Inc. on behalf of University of Washington. This is an open access article under the CC BY-NC-ND license. (http://creativecommons.org/licenses/by-nc-nd/4.0/)

Introduction

Chordomas have an incidence of 0.08/100,000 [1] and accounting for up to 4% of all bone tumors [2]. Typically, they are slow growing malignant tumors that can arise anywhere along the neuronal axis, and are very rare in those younger than 20 years [2]. Unlike adults, the majority of pediatric chordomas are intracranial (up to 54% [2]), centered around the spheno-occipital synchondrosis, with an average age of diagnosis around 10 years and no gender predilection [2]. Metastatic disease is rare at presentation in all age groups, although more common

in sacro-coccygeal tumors (approximately 25%) than in clival chordomas, with the lung as the primary site of metastasis [1,3].

Case report

A 9-year-old Caucasian male presented with a 3-month history of diplopia, morning headaches, nausea, vomiting, neck pain, and a 20 lbs weight loss. Physical examination revealed anisocoria and a left abducens nerve palsy.
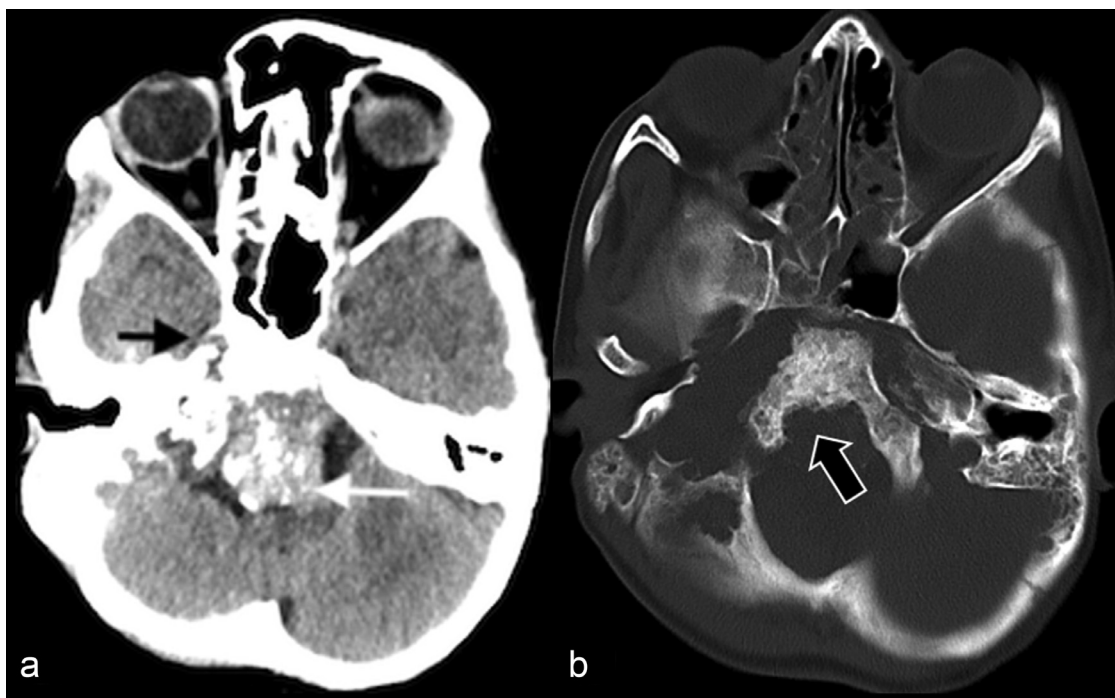
Fig. 1 – Axial noncontrast CT soft tissue window (a) at the level of skull base in 9-year-old boy with pathology proven chordoma shows erosions of right petrous bone and adjacent clivus (black arrow), with a large intracranial soft tissue mass compressing the brain stem, with extensive calcifications (white arrow). (b) Axial CT bone window at the level of clivus shows the destructive clival bony lesion with cortical erosions and hyperostosis (arrow).

The remaining neurologic exam was unremarkable. CT head and cervical spine was initially performed and revealed a large hyperdense posterior skull base mass with calcifications eroding the clivus, bilateral petrous bones, right jugular foramen, right occipital condyle, tip of dens process, and anterior arch and right lateral mass of C1 with an intraspinal soft tissue component (Figs. 1 and 2). A large extraosseous prevertebral soft tissue component was also present, causing near complete obstruction of the nasopharynx (Fig. 2).

Brain MRI revealed a large T1WI hypointense, T2WI hyperintense clival mass with heterogenous enhancement after gadolinium administration (Figs. 3 and 4). Most of the lesion had facilitated diffusion with a single focus of mild restricted diffusion. There was extensive mass effect on the pons, medulla, right cerebellar tonsil, and fourth ventricle by the large intracranial component (Fig. 4) resulting in moderate supratentorial ventriculomegaly and/or hydrocephalus with mild periventricular interstitial edema (Fig. 5).

Whole spine MRI performed as part of the initial staging showed no subarachnoid intraspinal metastasis; however, multiple lung nodules suggesting metastases were incidentally detected and later confirmed by chest CT (Fig. 6). Pathology specimen of the skull base lesion showed neoplastic proliferation composed of nests and cords of eosinophilic epithelioid cells and physaliphorous cells embedded predominantly in a chondroid-like matrix, consistent with chondroid chordoma (Fig. 7).

Discussion

Chordomas arise from notochord remnants, spheno-occiptal (35%) and sacrococcygeal regions (55% [1]) are the most common locations in adults. The average age at diagnosis is 58 years, with a male predominance [4]. Children under the age of 5 years tend to present with more aggressive disease and worse prognoses. Chordomas typically are locally aggressive, with distant metastasis occurring in 7%-43% of adults [2], most commonly to the lungs [1,3]. Other sites include liver, bone, soft tissue, and lymphatics [3,5,6]. Less than 5% of all patients present with metastases at diagnosis [2], but metastases are seen in up to 25% of sacrococcygeal tumors [1].

Metastases are relatively common in children, especially under the age of 5 years, with 8.6%-58% of children developing metastatic disease [2,5]. Metastases in chordomas are more common with local recurrence and highly unusual at the initial presentation [6]. Our patient presented with a clival chordoma and lung metastases at the initial presentation at 9 years of age.

Clinical manifestations depend on the location of the tumor. Sacral chordomas present with nonspecific back pain, and bowel or bladder dysfunction [5]. Clival chordomas present with cranial nerve palsies, visual disturbances, headaches, and elevated intracranial pressure, particularly in children under the age of 5 years [5,7]. Our patient presented with diplopia, morning headaches, abducens nerve palsy, and extracranial tumor extension to C1/C2.
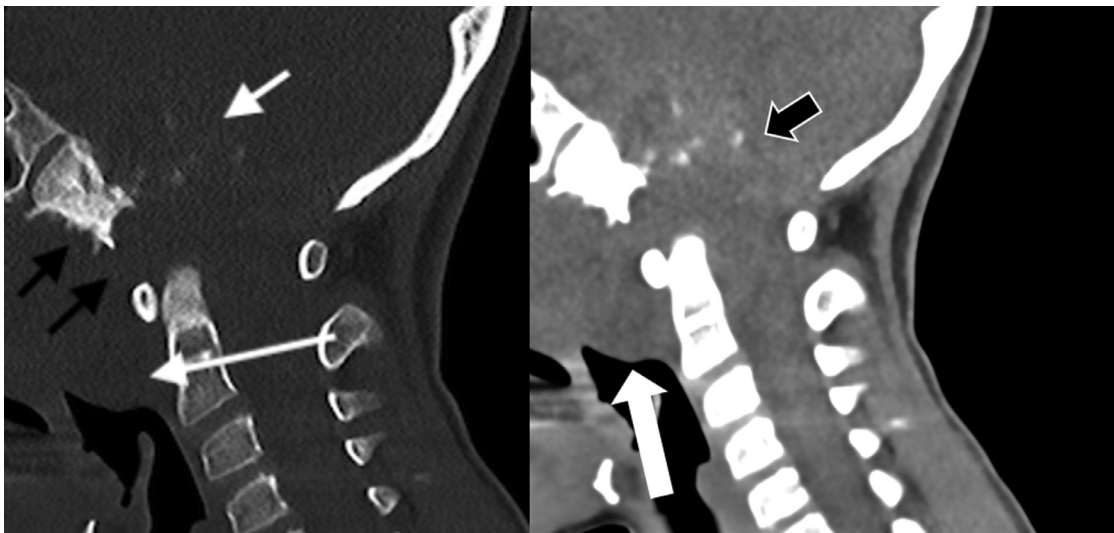
Fig. 2 – Midline sagittal CT bone window (a) at the craniocervical junction shows a large destructive clival bony lesion (black arrows) with scattered calcific foci (white short arrow). The mass extends into nasopharynx and retropharyngeal spaces (white long arrow). (b) Midline sagittal noncontrast CT soft tissue window at the same level shows the large destructive clival bony lesion with hyperdense extraosseous intracranial soft tissue component with scattered calcific foci (wide black arrow). The nasopharyngeal soft tissue component is seen compromising the nasopharyngeal air way (wide white arrow).

Fig. 3 – Axial Spin Echo Acquisition T2W images (1.5 T, TR/TE = 5650/96 ms, Slice thickness = 4 mm) shows hyperintense signal intensity of the lesion and mass effect on the brain stem. There is mass effect on and displacement of right vertebral artery (black arrow) with mass effect on the right internal jugular vein (white arrow).

Clinical course and treatment for clival chordomas include maximum surgical resection, followed by high-dose and high-precision radiotherapy [2,5]. Though histologically low grade, the recurrence rate is high, ranging from 26.7% to 66.7% [2] even with surgical resection and radiation, so complete surgical resection is crucial for long-term control [2,8]. Recently treatment has focused on prognostic stratification based on location, and protein and genetic biomarkers, such as brachyury [8]. Our patient underwent transnasal debulking surgery with ventriculoperitoneal shunt placement followed by lateral and/or upper cervical approach resection of the skull base chordoma with suboccipital craniotomy which was then followed by radiation therapy.

CT and MRI offer complimentary information in the diagnoses of chordomas. CT can be used for diagnosis and evaluation of bony destruction of the skull base that is characteristic of clival chordomas [4,5]. On CT, a clival chordoma is a hyperdense, well demarcated, soft tissue mass with marked postcontrast enhancement [4]. Chordomas appear heterogeneous and isodense in bone windows due to interspersed tumor, with hypodense areas of necrosis from bony destruction [5]. MRI with contrast is helpful for diagnosis and surgical planning. MRI is sensitive for the determination of the extent of soft tissue invasion, vascular, cranial nerve involvement, postoperative changes, and tumor recurrence. Chordomas may appear lobulated, hypointense on T1W, and hyperintense on T2W due to the high fluid content [4]. Chordomas may also show a distinctive lobulated honeycombing appearance of the septae after the administration of gadolinium contrast [5].

Differential diagnoses are particularly broad in the pediatric population and includes chondrosarcoma, benign notochord tumors, giant cell tumor, Ewing sarcoma, lymphoma, nasopharyngeal carcinoma, and rhabdomyosarcoma
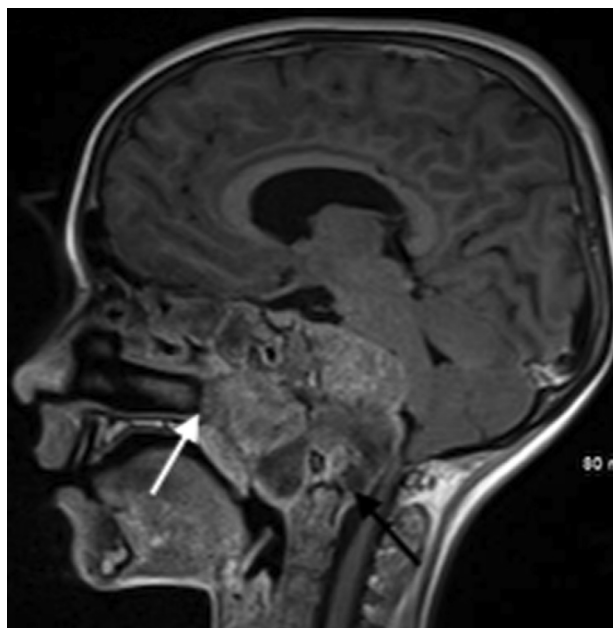
Fig. 4 – Post contrast midline Sagittal 3D SPACE T1 W images (1.5 T, TR/TE = 600/7.2 ms, Slice thickness = 1mm) shows a large heterogeneously enhancing clival mass with intracranial extension compressing the brainstem and nasopharyngeal extension compressing the nasopharyngeal airway (white arrow). There is intraspinal and retropharyngeal extension to C1-C2 level (black arrow).
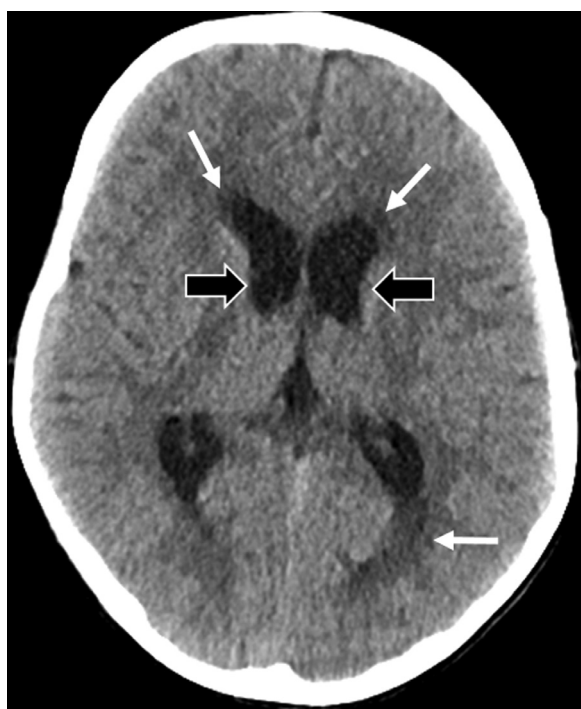

Fig. 5 – Axial noncontrast CT demonstrates dilated frontal horns and trigones of lateral ventricles (wide black arrows) with bilateral periventricular interstitial edema (white arrows), characteristic of hydrocephalic changes.
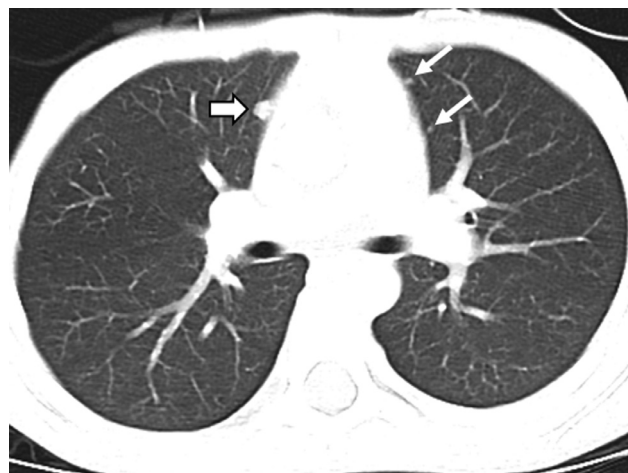

Fig. 6 – Axial CT images of the chest, lung window demonstrates well defined ovoid subpleural pulmonary nodule within the medial segment of the middle lung lobe (wide arrow). Two subpleural tiny pulmonary nodules are also noted within the inferior lingual segment of left upper lung lobe (white arrows).
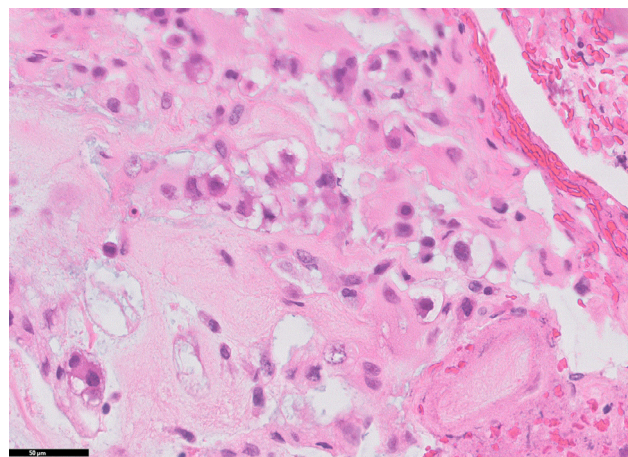

Fig. 7 – Pathology slide of the skull base chondroid chordoma shows neoplastic proliferation of nests and cords of eosinophilic epithelioid cells and physaliphorous cells embedded in a chondroid-like matrix. The significant presence of this chondroid-like matrix is characteristic of the so-called chondroid chordoma. Areas of necrosis are seen, but no poorly differentiated focus or areas of anaplasia are observed.

[7]. Chondrosarcomas arise in a similar location and show similar MR signal, but are more likely to have globular or linear calcifications [5] as opposed to arch-like [7]. Pathologically, Brachyury is expressed in chordomas, not chondrosarcomas [5]. Nasopharyngeal tumors extend more anteriorly and have associated lymphadenopathy [7]. Lymphoma is associated with lymphadenopathy, unusual clival destruction and reduced diffusion. Ewing sarcoma, which is more common than chordomas, can cause bony destruction, a hypercellular soft

tissue component with reduced diffusion, and lung metastases.

Clival involvement of the tumor may appear as a characteristic "thumb" of tissue extending posteriorly into and distorting the surface of the pons [4]. Local destruction of the clivus, which can be appreciated on CT and MRI as intratumoral calcification, and extradural compression are characteristic features of chordomas in patients less than 5 [5].

Conclusion

Chordomas are slow growing neoplasms that are particularly uncommon in patients under 20 years. When faced with lung nodules combined with the presences of a clival mass in pediatric population, a chordoma should be considered in a radiologist's differential diagnosis.

REFERENCES

[1] Ikpeze T, Mesfin A. The top 50 cited articles on chordomas. J Spine Surg 2018;4(1):37–44. doi:10.21037/jss.2018.03.13 https://www.ncbi.nlm.nih.gov/pmc/articles/PMC5911749/.

[2] Habrand JL, Datchary J, Bolle S, Beaudré A, de Marzi L, Beccaria K, Dendale R. Chordoma in children: case-report and review of literature. Rep Pract Oncol Radiother 2016;21(1):1–7. doi:10.1016/j.rpor.2015.10.007 https://www.sciencedirect.com/science/article/pii/S1507136715001406?via%3Dihub.

[3] Virdi G, McGraw I, MacDuff E, Periasamy K, Sharma H. An atypical presentation of chordoma: case report and review. Orthop Muscular Syst 2017;6:247. doi:10.4172/2161-0533.1000247.

[4] Chauhan A, Ahluwalia VV, Saharan PS, Sharma N, Narayan S, Gupta R. Clival chordoma in a young child. Appl Radiol 2017;46(11):37–41. https://appliedradiology.com/articles/clival-chordoma-in-a-young-child.

[5] Beccaria K, Sainte-Rose C, Zerah M, Puget S. Paediatric Chordomas. Orphanet J Rare Dis 2015;10:116. doi:10.1186/s13023-015-0340-8. https://www.ncbi.nlm.nih.gov/pmc/articles/PMC4578760/.

[6] Young V, Curtis KM, Temple HT, Eismont F, DeLaney T, Hornicek F. Characteristics and patterns of metastatic disease from chordoma. Sarcoma 2015. doi:10.1155/2015/517657 http://downloads.hindawi.com/journals/sarcoma/2015/517657.pdf.

[7] Géhanne C, Delpierre I, Damry N, Devroede B, Brihaye P, Christophe C. Skull base chordomas: CT and MRI features. JBR BTR 2005;88:325–7. https://www.researchgate.net/profile/Benoit_Devroede/publication/7332226_Skull_base_chordoma_CT_and_MRI_features/links/0fcfd50b371d1783d6000000.pdf.

[8] Sahyouni R, Goshtasbi K, Mahmoodi A, Chen JW. "A Historic Recount of Chordoma. J Neurosurg Spine 2018;28:422–8.